

Hydrodynamic Motion of a Heavy-Ion-Beam-Heated Plasma

J. Jacoby,^{(1),(a)} D. H. H. Hoffmann,⁽¹⁾ R. W. Müller,⁽¹⁾ K. Mahr-Olt,^{(1),(2)} R. C. Arnold,^{(1),(3)}
V. Schneider,^{(1),(4)} and J. Maruhn^{(1),(4)}

⁽¹⁾*Gesellschaft für Schwerionenforschung (GSI), D-6100 Darmstadt, Federal Republic of Germany*

⁽²⁾*Max Planck Institut für Quantenoptik (MPQ), D-8046 Garching, Federal Republic of Germany*

⁽³⁾*Institut für Angewandte Physik, TH-Darmstadt, D-6100 Darmstadt, Federal Republic of Germany*

⁽⁴⁾*Institut für Theoretische Physik, Universität Frankfurt, D-6000 Frankfurt, Federal Republic of Germany*

(Received 16 May 1990)

The first experimental study is reported of a plasma produced by a heavy-ion beam. Relevant parameters for heating with heavy ions are described, temperature and density of the plasma are determined, and the hydrodynamic motion in the target induced by the beam is studied. The measured temperature and the free-electron density are compared with a two-dimensional hydrodynamic-model calculation. In accordance with the model, a radial rarefaction wave reaching the center of the target was observed and the penetration velocity of the ion beam into the xenon gas target was measured.

PACS numbers: 52.40.Mj, 52.35.Tc, 52.50.-b

Intense heavy-ion beams are an important alternative tool to generate high-energy density in matter.¹⁻⁴ Because of their energy deposition profile, heavy ions create a heated volume, rather than a heated surface. This enables an effective coupling of a beam to a target. The new accelerator facility SIS at GSI (a heavy-ion synchrotron) will soon be able to provide intense beams of heavy ions which can generate plasmas at solid densities. The production and analysis of these plasmas is a first step to investigate the potential of heavy ions as a driver for inertial confinement fusion.³⁻⁵

As an initial step, the development of radio-frequency quadrupole (RFQ) accelerators for heavy ions at low energies allows the production of beams with low emittance and high current. Using the RFQ preaccelerator⁶ MAXILAC at GSI and a gas target, the investigation of a plasma produced by a heavy-ion beam recently became possible. The hydrodynamic behavior of beam-heated plasmas is complex, and therefore analyzing and modeling of such plasmas is an important test of the present understanding in this new field of beam-plasma interaction. The purpose of this Letter is to describe the first experiment where such a plasma is studied,⁷ showing by visible-light emission the effects of hydrodynamic motion in the target induced by the beam.

Parameters.—The main relevant parameter for heating a given target material with heavy ions is the specific deposition power P , the deposited power of the beam in a target per mass unit. P is calculated from the particle energy E of the accelerated ions, the range of the ions R , the particle current I , and the spot area a , as

$$P = 0.1(E/R)I/a, \quad (1)$$

where P is in GW/g, E is in MeV, R in mg/cm², I in particle mA, and a in mm². In our experiment using Kr⁺ ions, we obtained $E = 3.8$ MeV, I up to 5 mA, and $a \approx 1$ mm². For the stopping of heavy ions in the MeV

energy range both electronic stopping and nuclear stopping contribute a comparable amount. The energy loss is nearly constant along the ion path. Values for the range R in cold matter are tabulated by Northcliffe and Schilling.⁸ The plasma temperature is maximized by using a heavy element as target material. We chose xenon gas which yields for the values given above the specific deposition power $P = 1.5$ GW/g, and with a range $R = 1.28$ mg/cm².

The other important parameter for determining the temperature is the maximum effective heating time for a target. The hydrodynamical limit⁹ for this time can be derived for an unconfined (open) target with the following simple model: A cylindrical target volume is heated homogeneously by a uniform ion beam. The pressure gradients at the boundary of the heated volume generate an outward-moving compression wave and an inward-moving rarefaction wave. The thermal energy then is converted to kinetic energy and the heating is counteracted by the expansion. The time t_h when the rarefaction wave reaches the center of the heated volume determines the hydrodynamical limit for heating. The velocity of the rarefaction wave is roughly the sound velocity c_T . Since the specific energy of the target ϵ (the energy per mass) is given for a gas by the square of the sound velocity $\epsilon = c_T^2 = Pt$, the integral

$$r_0 = \int_0^{t_h} c_T dt = \frac{2}{3} P^{1/2} t_h^{3/2}, \quad (2)$$

with r_0 the radius of the heated region, yields an expression for the hydrodynamic expansion time t_h of the heated matter:

$$t_h = (9r_0^2/4P)^{1/3}. \quad (3)$$

For our parameters, with $r_0 = 1$ mm, Eq. (3) yields $t_h = 1.1$ μ s. The maximum specific energy ϵ_{\max} is estimated from $\epsilon_{\max} = Pt_h$. With a rough approximation⁹

for the equation of state for high- Z material $\epsilon \cong \epsilon_0 T^{4/3}$, the maximal temperature is then calculated as

$$T_{\max} \cong f \left(\frac{3}{2} P r_0 \right)^{1/2}, \quad (4)$$

where f is a material-dependent constant (with P in GW/g and r_0 in mm, $f \approx 0.5$ eV).⁹ This yields $T_{\max} \approx 0.8$ eV.

Experimental setup.—Singly charged krypton ions are accelerated with the RFQ preaccelerator MAXILAC to 45 keV/u. A current of 4–5 mA Kr^+ during a macropulse of 0.5–2 ms is obtained. A special ion optical system¹⁰ for singly charged Kr ions was developed to focus the beam to a small spot, to maximize the specific deposition power [Eq. (1)]. The main part of the fine focusing lens consists of two electrostatic quadrupoles which focus the ion beam to a spot 7 cm after the last quadrupole. An elliptical spot (axis ratio 1:4) with approximately 1-mm² spot area is created. An electrostatic kicker is placed between the two electrostatic quadrupoles. The kicker deflects the beam onto a beam dump during the slow rise time of the RFQ macropulse (≈ 50 μs). In order to optimize the heating of the gas, the beam has to be switched on in a time much less than the hydrodynamical expansion time t_h [Eq. (3)]. After the maximum beam intensity is reached, the ion beam is kicked within 100 ns onto the target. The switching off is not perfect because of a beam halo. Only 90%–95% of the beam intensity is stopped at the beam dump. Some of the remaining beam then causes preheat in the target.

The closed-cell gas target¹¹ is the target type best suited to study the hydrodynamic motion inside the heated material. The initial conditions are homogeneous and stationary, and the penetration depth of the ions can be adjusted by changing the gas density to be larger than the diameter of the beam spot. This optimizes t_h [Eq. (3)], which is determined by the smallest distance to the center of the heated volume. A quartz tube, shown in Fig. 1 (length 12 mm, inner diameter 6.5 mm), was filled

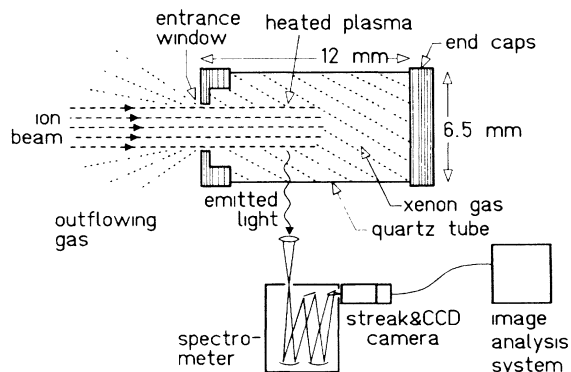


FIG. 1. Diagram of the quartz-tube target during the heating with the Kr^+ beam. The beam is focused to the entrance window on the left side of the tube. The entrance foil is destroyed and the heated xenon is released into the vacuum.

with xenon gas at an initial pressure of 0.6 bar. The entrance of the tube to the vacuum is sealed by a polypropylene foil with a thickness of less than 1 μm (≈ 80 $\mu\text{g}/\text{cm}^2$). This is about one-third of the range of the ions. The entrance foil is destroyed early in the pulse during every shot. The entrance window of this target is adapted to the elliptical shape of the beam spot.

Diagnostics and results.—The light from the target (Fig. 1) is detected with a photodiode, providing a reference signal to compare different shots and to estimate the emitted power in the visible spectrum. A spectrometer connected to a streak camera provided a time-resolved measurement of the radiation in the 200–800-nm wavelength region. A quartz lens is used to focus the emitted light onto the slit of the spectrometer. The spectra are taken from the center of the tube.

The electron density is determined by analyzing the Stark broadening of two XeI lines (467.1 nm, 462.4 nm). The half-widths for these lines are tabulated¹² in a density region of $n_e = (2-10) \times 10^{16}$ cm^{-3} and for temperatures from 9000 to 12500 K. According to our estimation,⁷ other physical broadening mechanisms like Doppler broadening or self-absorption are negligible. The instrumental resolution of the spectrometer (0.2 nm) was taken into account. The measured electron density reached is maximum of $n_e = (5 \pm 1) \times 10^{16}$ cm^{-3} after about 3 μs heating time. During the next 15 μs this value decreased to $n_e = (3 \pm 1) \times 10^{16}$ cm^{-3} .

The temperature is determined from the line ratios of a XeI (467.1 nm) with a XeII (460.3 nm) line. Following to the general estimates of Griem,^{7,13} local thermodynamic equilibrium for the relevant atomic levels is assumed. The maximum temperature of $T_e = 0.75 \pm 0.15$ eV is obtained after about 14 μs heating. Additional estimates of the plasma temperature from the velocity of reflected shock waves and from a determination of the degree of ionization (using n_e and the Saha equation) were consistent with the spectroscopic results.

The space- and time-resolved behavior of the emission is studied by using the streak camera without spectral resolution. The slit of the streak camera is aligned in this case along the central axis of the tube, and the penetration of the ion beam into the gas target is observed. A two-dimensional streak image taken in this geometry records the behavior of the emitted light versus time along the z axis of the quartz tube.

Figure 2 represents three traces of such a streak image for a given position at the axis versus time. The beam is switched on at time zero and penetrates initially 3.7 mm at 0.6-bar xenon pressure along the z axis into the target ($R = 1.28$ mg/cm^2). All three curves are taken from positions downstream from this initial penetration. The observed light intensity starts from a background preheat level, due to the imperfect kicking of the ion beam, and increases during about 1.4 μs (at $z = 4.2$ mm) 1 order of magnitude to a first maximum. In Fig. 2 we have indicated the position of this maximum. Traces with a

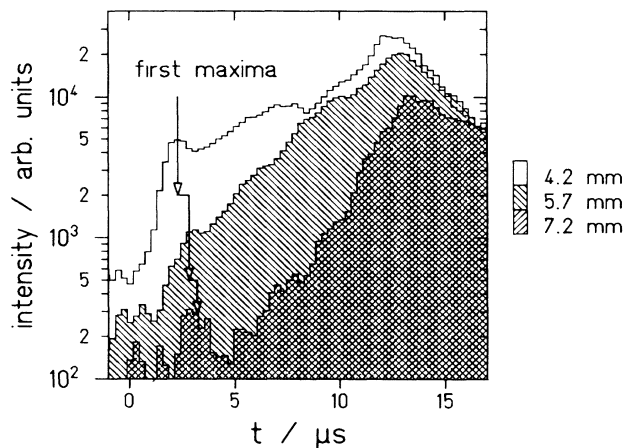


FIG. 2. Traces of a two-dimensional space-resolved streak image. The three curves correspond to fixed z positions along the axis; the abscissa is time. The ion beam is switched on at time zero and penetrates initially 3.7 mm into the 0.6-bar xenon gas.

higher- z value further downstream start at later times. This first maximum is detected very reliably in the two-dimensional streak images during these measurements. The intensity of the first maximum decreases by a factor of 20, and the rise time to this maximum decreases by a factor of 2 with z increasing from 4.2 to 7.2 mm. About 14 μ s after this first maximum, the total maximum of the emission is observed for all three traces (Fig. 2).

The emitted light intensity increases with temperature and with particle density. When a rarefaction wave reaches the observed region the particle density decreases very rapidly; therefore the emitted light intensity drops and a relative emission maximum is created. This maximum (easily seen in Fig. 2) provides an experimental determination of the hydrodynamical expansion time t_h and is in very good agreement with t_h calculated from Eq. (3). The overall maximum of the emission curves is interpreted as the increasing emission due to a superposition of reflected shock waves.

If the position of the first detected light at the z axis of the tube is plotted versus time, taken from the rise to the first emission maximum for several traces similar to those in Fig. 2, a fast penetration into the target is observed. From a linear fit of these positions the penetration velocity $v_{in} = 1520 \pm 180$ m/s is determined. This process is according to the two-dimensional hydrodynamical model caused by the fast penetration of heavy ions into the target material. The rarefaction wave dilutes the target, whereas the range of the ions is not changed and, thus, the ions penetrate deeper into the target.

Theoretical model.—A two-dimensional model simulation was performed with the hydrodynamical code CONCHASPRAY.¹⁴ The code uses cylindrical coordinates for 30×50 elements of mass cells. Cylindrical

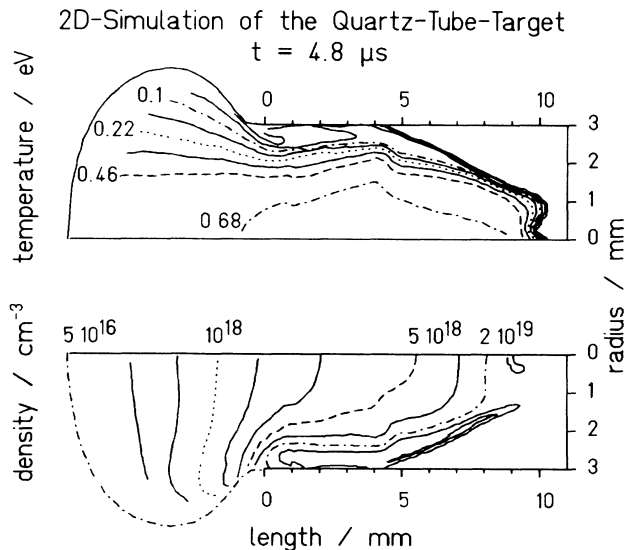


FIG. 3. Two-dimensional hydrodynamical-model calculation of the xenon tube target. Shown are contour lines of temperature (upper part) and density (lower part) after 4.8 μ s heating time.

symmetry is assumed. The inner volume of a xenon gas inside the beam radius ($r_0 = 1.5$ mm) is heated with a specific deposition power of 1.5 GW/g at an initial pressure of 0.6 bar. The tube radius is 3 mm. The deposition power is switched on linearly during 100 ns. A radial parabolic intensity profile of the deposition power is assumed. The entrance of the tube is assumed to be open to the vacuum.

Figure 3 shows the temperature and density distribution of such a simulation after 4.8 μ s heating time. The calculation starts from a homogeneous density and temperature distribution. At the beginning a rectangular profile of contour lines is created with a penetration depth of 3.7 mm and at a beam radius of 1.5 mm. From the boundary of this profile then an outward-moving compression wave and an inward-going rarefaction wave are created. Because of this mass flow the density inside the inner volume decreases and the ion beam penetrates further into the target.

The simulation shows that during 4.8 μ s the compression shock wave propagates from the inner heated volume almost up to the walls of the tube. During this time the beam penetrates about 6 mm into the target. The estimated penetration velocity in the model calculation is $v \approx 1250$ m/s. The downstream beam penetration, according to the model, is caused by the rarefaction of upstream target material heated at earlier times by the beam. For this simulation, neglecting energy loss due to radiation, the temperature reaches after 4.8 μ s a maximum of $T_e = 0.68$ eV in the center of the target. For a calculation with radiative energy loss the central temperature after this time is about 0.15 eV lower, if a

Planck mean opacity of $10^4 \text{ cm}^2/\text{g}$ is assumed.

The two-dimensional simulation was not extended to longer times because of large computing time requirements. However, one-dimensional (radial) simulations were carried out which predict secondary maxima of the light emission beginning at about $7 \mu\text{s}$, from compression waves reflected back to the axis. We interpret the overall maxima in Fig. 2 as a superposition of such reflections.

In conclusion, this experiment is the first investigation of a heavy-ion-beam-produced plasma. The comparison of experiment and hydrodynamic-model calculations shows good agreement of measured and calculated temperature and density in the center of the target. During this experiment, characteristic phenomena such as the hydrodynamic motion governing the ion beam penetration into the target were observed.

The measured penetration velocity v_{in} is in satisfactory agreement with the estimated velocity from the two-dimensional model. The detected decrease, however, of the first emission maximum (Fig. 2) by a factor of 20 between $z=4.2$ and 7.2 mm is not in agreement with the simulation. Apparently only a part of the ion beam penetrates with this fast velocity. We interpret this to mean that the plasma density is not as uniform as in the simulations; there is additional hydrodynamic complexity, possibly because of the highly elliptical focus spot.⁷

The detection of the rarefaction wave reaching the center provided an experimental determination of the hydrodynamic expansion time [Eq. (3)]. This method of hydrodynamic determination of the plasma temperature is likely to be useful in further investigations of near

solid density plasmas generated by high-energy beams, e.g., from SIS at GSI.

This work was supported by the Bundesministerium für Forschung und Technik (BMFT) of the Bundesrepublik Deutschland.

^(a)Present affiliation: Max Planck Institut für Quantenoptik, D-8046 Garching, Federal Republic of Germany.

¹R. C. Arnold, *Nature (London)* **276**, 19 (1978).

²R. Bock, *Phys. Bl.* **37**, 214 (1981).

³R. C. Arnold and J. Meyer-ter-Vehn, *Rep. Prog. Phys.* **50**, 559 (1987).

⁴C. Deutsch, *Ann. Phys. (Paris)* **11**, 1 (1986).

⁵B. Badger *et al.*, Kernforschungszentrum Karlsruhe Report No. KfK-3940, 1985 (unpublished).

⁶R. W. Müller *et al.*, GSI Scientific Report No. GSI-86-1, 1985, 1986 (unpublished), p. 375.

⁷J. Jacoby, thesis, Universität Heidelberg, Report No. GSI-89-24 (unpublished).

⁸L. C. Northcliffe and R. F. Schilling, *Nucl. Data, Sect. A* **7**, 233 (1970).

⁹R. C. Arnold and J. Meyer-ter-Vehn, *Z. Phys. D* **9**, 65 (1988).

¹⁰B. Heimrich, thesis, Universität Giessen, Report No. GSI-89-7 (unpublished).

¹¹J. Jacoby, *Nucl. Instrum. Methods Phys. Res., Sect. A* **282**, 94 (1989).

¹²Truong-Bach, J. Richou, A. Lesage, and M. H. Miller, *Phys. Rev. A* **24**, 2550 (1981).

¹³H. Griem, *Plasma Spectroscopy* (McGraw-Hill, New York, 1964).

¹⁴V. Schneider and J. Maruhn, *Laser Part. Beams* **7**, 807 (1989).